

Compressed Video Quality Enhancement with Temporal Group Alignment and Fusion

Qiang Zhu, Yajun Qiu, Yu Liu, Shuyuan Zhu, *Member, IEEE*, Bing Zeng, *Fellow, IEEE*

Abstract—In this paper, we propose a temporal group alignment and fusion network to enhance the quality of compressed videos by using the long-short term correlations between frames. The proposed model consists of the intra-group feature alignment (IntraGFA) module, the inter-group feature fusion (InterGFF) module, and the feature enhancement (FE) module. We form the group of pictures (GoP) by selecting frames from the video according to their temporal distances to the target enhanced frame. With this grouping, the composed GoP can contain either long- or short-term correlated information of neighboring frames. We design the IntraGFA module to align the features of frames of each GoP to eliminate the motion existing between frames. We construct the InterGFF module to fuse features belonging to different GoPs and finally enhance the fused features with the FE module to generate high-quality video frames. The experimental results show that our proposed method achieves up to 0.05dB gain and lower complexity compared to the state-of-the-art method.

Index Terms—Compressed video, quality enhancement, long-short term, feature, correlation.

I. INTRODUCTION

COMPRESSION artifacts normally occur in the compressed video due to the lossy coding, sometimes resulting in serious quality degradation [1]–[3]. To address this issue, compressed video quality enhancement has been developed to construct high-quality (HQ) video from the compressed low-quality (LQ) one.

Over the past decades, lots of methods have been proposed to implement compressed video quality enhancement. These methods achieve impressive quality improvement, not only for the 2D video [4]–[6] but also for the 3D video [7], [8]. Among these methods, the single-frame-based enhancement methods [4]–[6] were firstly proposed and they utilized an LQ frame to generate HQ frame. Although these methods improved quality for compressed videos, they ignored using the temporal correlation of neighboring frames to construct the enhancement models, which limits their performance.

To achieve high enhancement performance, the multi-frame-based enhancement methods [9]–[15] were proposed and the optical flow is often used in these methods to construct temporal correlation between frames for the producing of HQ videos. For instance, the multi-frame quality enhancement (MFQE) [9] was firstly proposed to use convolution neural network (CNN) to estimate the optical flow of the local high-quality frame and the target frame. With the flow, the temporal correlation of frames was constructed in MFQE, which makes the model achieve high performance. In addition, a multi-scale

motion compensation network was designed in MFQE 2.0 [10] to utilize the multi-scale optical flow to generate the motion-compensated feature for removing compression artifacts. However, if there exist large motions in video, it is difficult to obtain accurate flow, which limits the enhancement efficiency. Recently, the spatio-temporal deformable fusion (STDF) [11] was proposed for compressed video quality enhancement. It adopts the deformable convolution network (DCN) [22] to explore temporal information than optical flow from the video and accordingly achieves significant performance improvement. Later on, the recursive fusion and deformable spatiotemporal attention (RFDA) [12] based method [11] was designed to exploit long-range spatio-temporal information and to pemploy the deformable spatiotemporal attention based on DCN for the construction of HQ videos. Recently, spatio-temporal detail information retrieval network [13] was constructed to utilize DCN with different receptive fields to compose temporal detail information for quality enhancement.

In addition to the DCN-based methods, the attention-based methods were also proposed to improve the quality of compressed videos [14] or the super-resolved videos [16], [17]. For instance, both spatio-temporal attention and channel attention were adopted in [14] to exploit correlation of multiple frames for generation of HQ videos. The deformable attention was employed in [16] to finely fuse features of adjacent frames for the generation of high-quality video. The temporal difference attention was proposed in [17] based on temporal difference learning to explore motions from video and then to compensate them to target frame for the enhancement of video quality. However, the above methods disregard the utilization of the long and short terms correlations between frames, which limits their efficiency to obtain effective temporal features for the composition of high-quality videos.

In this paper, we propose a temporal group alignment and fusion network (TGAFNet) for the quality enhancement of compressed videos according to the long-short term correlations between frames. It is a post-processing method like [10]–[12] and just carried out at decoder side. Our proposed model consists of the intra-group feature alignment (IntraGFA) module, the inter-group feature fusion (InterGFF) module and feature enhancement (FE) module. The temporal grouping strategy has demonstrated high feature alignment performance for quality improvement of super-resolved video [18]. Inspired by this, we also adopt this strategy in our proposed method. Specifically, we firstly select the frames from video to form group of pictures (GoP) according to the temporal distances to the target enhanced frame. Then, the IntraGFA module is applied to align the features of frames of each GoP to eliminate the motion error. After that, the aligned features of different GoPs are fed into the InterGFF module to gradually fuse the aligned features to produce the temporally-fused features for

The authors are with School of Information and Communication Engineering, University of Electronic Science and Technology of China, Chengdu 611731, China. This work was supported by the National Natural Science Foundation of China under Grant U20A20184, in part by the Natural Science Foundation of Sichuan Province under Grant 2023NSFSC1972, 2022NSFSC0509, and in part by CAAI-HuaweiMindSpore Open Fund under Grant CAAIXSJLJJ-2022-060A.

the construction of high-quality video frame. Finally, the FE module which is constructed based on our proposed spatial dual contextual block is applied to enhance the features for the generation of detailed video contents.

II. PROPOSED METHOD

The architecture of our proposed model, namely TGAFNet, is illustrated in Fig. 1 and it consists of the IntraGFA, InterGFF and FE modules. Given an LQ video $S = \{\dots, I_{k-N}, \dots, I_{k-1}, I_k, I_{k+1}, \dots, I_{k+N}, \dots\}$, we aim to produce the HQ frame Y_k for the target frame I_k according to the long-short term correlations between I_k and its neighbors.

To achieve the above goal, we firstly form N GoPs for each I_k with I_k and some of its neighbors, where GoP is formed as $G_i = \{I_{k-i}, I_k, I_{k+i}\}$, $i = 1, 2, \dots, N$. The neighboring frames of I_k in each G_i are selected according to their distances to I_k . In this work, we specify $N=3$ and three groups G_1 , G_2 and G_3 are formed for each I_k , as illustrated in Fig. 1. In order to achieve the effective enhancement for I_k , we construct the IntraGFA module and InterGFF module to align and fuse features so that we can enhance the quality of compressed video by effectively using the long-short term correlations between frames. In addition, we design the FE module to enhance features to compose high-quality video frames.

In our work, the IntraGFA module is firstly applied to align the features of the frames belonging to each G_i . According to the temporal distances of neighboring frames to I_k , we design the IntraGFA module based on DCN [22] with different kernel size K to extract features. In this work, we specify that $K = 1, 3$, and 5 for G_1 , G_2 , and G_3 , respectively. After obtaining features, we align them in each GoP to eliminate motion error within frames. Accordingly, the aligned features of each GoP are obtained as

$$\mathcal{F}^{(K)} = \text{IntraGFA}(G_i). \quad (1)$$

Then, we apply the InterGFF module to fuse the aligned features to obtain the temporally-fused feature as

$$\mathcal{F}_f = \text{InterGFF}(\mathcal{F}^{(1)}, \mathcal{F}^{(3)}, \mathcal{F}^{(5)}). \quad (2)$$

After that, \mathcal{F}_f is fed into the FE module to generate the enhanced feature

$$\mathcal{E}_k = \text{FE}(\mathcal{F}_f). \quad (3)$$

Finally, the HQ frame Y_k is obtained by fusing \mathcal{E}_k and the input frame I_k as

$$Y_k = \mathcal{E}_k + I_k. \quad (4)$$

A. Intra-group Feature Alignment

To implement the intra-group feature alignment, we construct the IntraGFA module based on U-Net [21] and DCN [22] to extract the features of frames of each GoP and align these features. Specifically, we firstly concatenate the frames of G_i to form f_{G_i} and apply U-Net, denoted as \mathcal{U}_{net} , to f_{G_i} to extract features. Then, a convolution layer is performed on the features to predict the deformable offset $\Delta\mathcal{O}_i$ for DCN. The offset $\Delta\mathcal{O}_i$ is obtained by using the intra-group offset convolutional network $\text{OCN}_{\text{intra}}$ as

$$\Delta\mathcal{O}_i = \text{OCN}_{\text{intra}}(\mathcal{U}_{net}(f_{G_i})) \in \mathbb{R}^{H \times W \times 6K^2}, \quad (5)$$

where $\text{OCN}_{\text{intra}}$ is composed by a convolution layer with $6K^2$ filters whose size is 3×3 , K is the kernel size of deformable convolution, and H and W are the height and width of feature, respectively. After that, the offset $\Delta\mathcal{O}_i$ is adopted in DCN to align f_{G_i} , generating the aligned features

$$\mathcal{F}^{(K)} = \text{DCN}^{(K)}(f_{G_i}, \Delta\mathcal{O}_i) \in \mathbb{R}^{H \times W \times C}, \quad (6)$$

where $\text{DCN}^{(K)}$ is the deformable convolution network whose kernel size is K , and C is the channel number of feature. With the IntraGFA module, the aligned features of $\mathcal{F}^{(1)}$, $\mathcal{F}^{(3)}$, $\mathcal{F}^{(5)}$ are generated for the corresponding three GoPs G_1 , G_2 , and G_3 . Due to the temporal distance-based grouping strategy, the aligned features in each GoP contain the short-term or long-term correlations between frames.

B. Inter-group Feature Fusion

To effectively utilize the long-short term correlations between frames to generate the effective features, we gradually fuse the aligned features to generate the temporally-fused feature. More specifically, we firstly fuse $\mathcal{F}^{(1)}$ with $\mathcal{F}^{(3)}$ and also fuse $\mathcal{F}^{(3)}$ with $\mathcal{F}^{(5)}$ to aggregate the temporal information of the neighboring groups to generate the fused features

$$\mathcal{F}^{(1-3)} = \text{Conv}([\mathcal{F}^{(1)}, \mathcal{F}^{(3)}]) \quad (7)$$

and

$$\mathcal{F}^{(3-5)} = \text{Conv}([\mathcal{F}^{(3)}, \mathcal{F}^{(5)}]), \quad (8)$$

where $[\cdot]$ is the concatenation operation and Conv is a convolution layer with C filters whose size is 3×3 and followed by a LeakyReLU activation function. Then, $\mathcal{F}^{(1-3)}$ and $\mathcal{F}^{(3-5)}$ are combined together to be sent into the residual channel attention block (RCAB) [27], forming the fused feature

$$\mathcal{F}_{fus} = \text{RCAB}(\text{Conv}[\mathcal{F}^{(1-3)}, \mathcal{F}^{(3-5)}]). \quad (9)$$

Next, we use the inter-group offset convolution network $\text{OCN}_{\text{inter}}$ and DCN to predict the deformable offset and align the fused feature to obtain the temporally-fused feature

$$\mathcal{F}_f = \text{DCN}^{(K)}(\mathcal{F}_{fus}, \text{OCN}_{\text{inter}}(\mathcal{F}_{fus})) \in \mathbb{R}^{H \times W \times C}, \quad (10)$$

where the kernel size of DCN is set as $K = 1$ and $\text{OCN}_{\text{inter}}$ consists of a convolution layer with $2CK^2$ filters whose size is 3×3 . With the InterGFF module, the fused feature is generated and it contains the long-term and short-term temporal information of the frames.

C. Feature Enhancement

We further enhance \mathcal{F}_f with the FE module so that we can use the enhanced feature to construct high-quality frame. The FE module is composed of $(L + 1)$ convolution layers with C filters whose sizes are all 3×3 and followed by a LeakyReLU activation function, L spatial dual contextual blocks, and a convolution layer, as illustrated in Fig. 1.

In the FE module, we design the spatial dual contextual block (SDCB) that implements the contextual module (CM) [28] in dual paths to exploit the spatially contextual information and strengthen the contextual information interaction to generate the contextually-enhanced feature. Some dual-path-based methods were proposed for face image hallucination [19] and image deraining [20]. However, they either lack

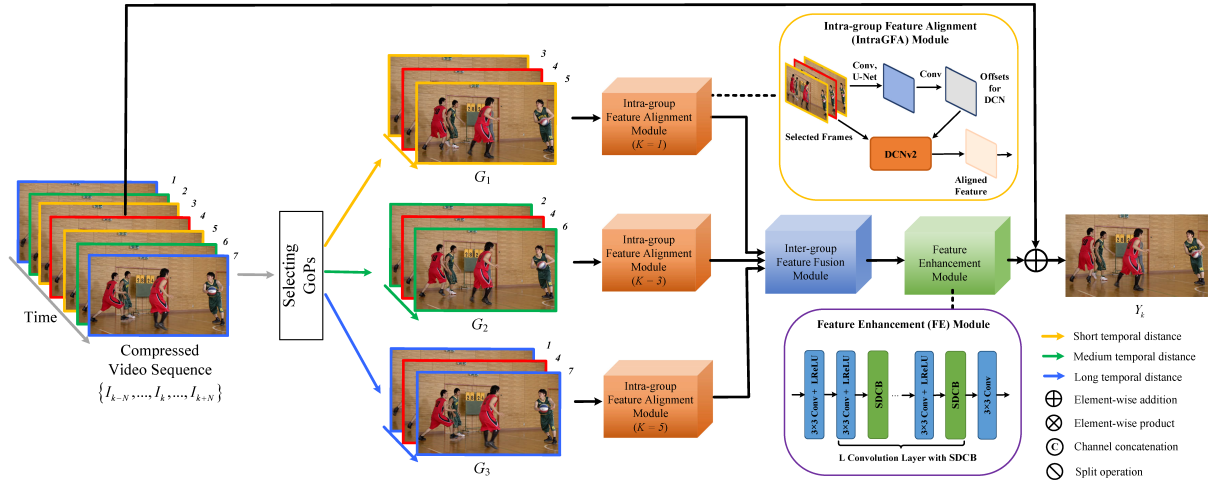


Fig. 1. The proposed model which consists of the InterGFA, IntraGFF and FE modules.

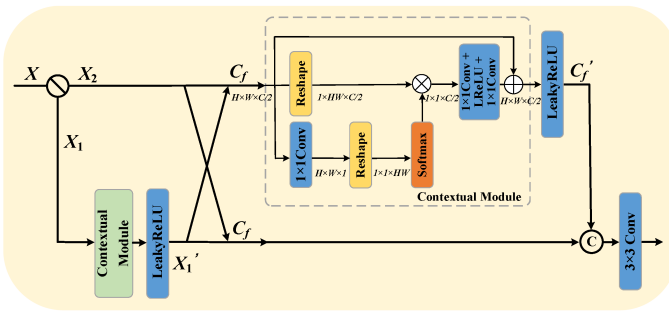


Fig. 2. Structure of SDCB.

information interaction between paths [19] or design complex interaction blocks [20], which limits their efficiency. In our method, we construct SDCB via simple skip connection to strengthen information interaction between paths without increasing model parameters, guaranteeing high enhancement performance with low complexity.

The architecture of SDCB is illustrated in Fig. 2. Specifically, the input feature $X \in \mathbb{R}^{H \times W \times C}$ is split into two features X_1 and $X_2 \in \mathbb{R}^{H \times W \times C/2}$. Then, X_1 is fed into one CM followed by a LeakyReLU activation function to obtain the contextual-aware feature X_1' . Next, X_1' is added to X_2 to obtain the feature $C_f \in \mathbb{R}^{H \times W \times C/2}$. After that, C_f is fed into another CM followed by a LeakyReLU activation function to obtain the contextual-aware feature C_f' . Finally, C_f' and C_f are fused via the concatenation and a convolution layer with C filters whose size is 3×3 to generate the enhanced feature.

III. EXPERIMENTAL RESULTS

1) *Experiment Setup*: Similar to [10]–[12], we conducted our experiments on MFQE2.0 dataset [10] that consists of 108 training videos and 18 testing videos of the Joint Collaborative Team on Video Coding [23]. All the videos are compressed by HM16.5 [24] under the LDP configuration. To evaluate the performance for different coding scenarios, the compression is carried out with 5 quantization parameters (QPs), i.e., 22, 27, 32, 37, and 42. Both the raw and compressed videos are cropped into 128×128 patches as the training pairs. We adopt flip and rotation as data augmentation techniques to expand the training dataset as [11] did. In addition, two quantitative

metrics PSNR and SSIM are used to evaluate the distortion on the luminance component as the previous work [10]–[12] did. For the network settings, 7 successive frames are used to construct the input sequence. The number of SDCB in the FE module is 3 and the channel number of feature is 64.

2) *Model Training*: We use the Charbonnier loss [29] to train our model. Additionally, the batch size is set to 32 and the learning rate is set to 1×10^{-4} . Our model is trained by Adam optimizer [25] with the exponential decay rates $\beta_1 = 0.9$ and $\beta_2 = 0.999$, the compensation factor $\varepsilon = 1 \times 10^{-8}$, and the total number of iterations is 3×10^5 . The proposed models are developed based on Pytorch with two NVIDIA GeForce RTX 3090 GPUs and Intel(R) Xeon(R) Gold 6133 CPU.

3) *Comparison to State-of-the-arts*: We compare our proposed method with one single-frame-based method, i.e., deep CNN-based auto decoder (DCAD) [5], and some multi-frame-based methods, i.e., MFQE [9], MFQE2.0 [10], STDF-R3L [11], RFDA [12], and coarse-to-fine spatio-temporal information fusion (CF-STIF) [26]. The results of Δ PSNR and Δ SSIM are presented in Table I, where the results of those compared approaches are offered by [12], [26]. It can be seen from Table I that our method offers the best performance in terms of Δ PSNR and Δ SSIM (on average), compared with these state-of-the-art methods on the testing videos at five QPs. Additionally, we present some visual results in Fig. 3 on testing compressed videos and real-world compressed videos to make a comprehensive comparison. The real-world videos were downloaded from YouTube with 1280×720 resolution. These results are obtained by using our proposed method and three competitive methods, i.e., STDF-R3L, RFDA and CF-STIF. It can be observed from Fig. 3 that compared with the other three methods, our method reduces more compression artifacts and achieves better visual results.

4) *Ablation Study*: We conduct the ablation study to validate the effectiveness of the IntraGFA, InterGFF and FE modules over all the test videos. In this experiment, we use the STDF module of STDF-R3L [11] as the baseline to enhance the compressed videos. The results of baseline method are presented in the first row in Table II. Because the IntraGFA and InterGFF modules can not separately work in our model, we combine them together to verify the effectiveness. The corresponding results are given in Table II. It is found from Table

TABLE I
COMPARISON RESULTS IN TERMS OF Δ PSNR (dB) AND Δ SSIM ($\times 10^{-4}$)

QP	Class	Sequence	DCAD		MFQE		MFQE2.0		STDF-R3L		RFDA		CF-STIF		Ours	
			PSNR	SSIM	PSNR	SSIM	PSNR	SSIM	PSNR	SSIM	PSNR	SSIM	PSNR	SSIM	PSNR	SSIM
37	A (2560 \times 1600)	Traffic	0.31	67	0.50	90	0.59	102	0.74	122	0.80	128	0.78	126	0.84	132
		PeopleOnStreet	0.50	95	0.80	137	0.92	157	1.25	202	1.44	222	1.40	216	1.53	233
		Kimono	0.28	78	0.50	113	0.55	118	0.91	173	1.02	186	0.99	181	1.06	194
	B (1920 \times 1080)	ParkScene	0.16	50	0.39	103	0.46	123	0.61	145	0.64	158	0.65	160	0.71	179
		Cactus	0.26	58	0.44	88	0.50	100	0.77	142	0.83	149	0.83	150	0.82	152
		BQTerrace	0.28	50	0.27	48	0.40	67	0.63	105	0.65	106	0.71	117	0.68	116
	C (832 \times 480)	BasketballDrive	0.31	68	0.41	80	0.47	83	0.80	134	0.87	140	0.88	143	0.92	150
		RaceHorses	0.28	65	0.34	55	0.39	80	0.52	116	0.48	123	0.59	154	0.64	164
		BQMall	0.34	88	0.51	103	0.62	120	0.90	186	1.09	197	1.11	197	1.13	207
	D (416 \times 240)	PartyScene	0.16	48	0.22	73	0.36	118	0.67	192	0.66	188	0.75	210	0.81	229
		BasketballDrill	0.39	78	0.48	90	0.58	120	0.79	146	0.88	167	0.94	173	0.89	171
		RaceHorses	0.34	83	0.51	113	0.59	143	0.81	194	0.85	211	0.91	227	0.97	248
	E (1280 \times 720)	BQSquare	0.20	38	-0.01	15	0.34	65	0.80	121	1.05	139	1.05	142	1.22	159
		BlowingBubbles	0.22	65	0.39	120	0.53	170	0.74	224	0.78	240	0.78	238	0.83	263
		BasketballPass	0.35	85	0.63	138	0.73	155	1.05	211	1.12	223	1.20	239	1.23	251
	Average	FourPeople	0.51	78	0.66	85	0.73	95	1.00	129	1.13	136	1.04	127	1.02	130
		Johnny	0.41	50	0.55	55	0.60	68	0.88	102	0.90	94	0.88	97	0.83	89
	Average	KristenAndSara	0.52	70	0.66	75	0.75	85	1.05	111	1.19	115	1.10	108	1.11	113
		Average	0.32	67	0.46	88	0.56	109	0.83	153	0.91	162	0.92	167	0.96	177
	42	Average	0.32	109	0.44	130	0.59	165	0.74	199	0.82	220	0.89	232	0.92	236
32	Average	0.32	44	0.43	58	0.52	68	0.86	107	0.87	107	0.95	118	1.00	126	
27	Average	0.32	30	0.40	34	0.49	42	0.77	64	0.82	68	0.94	78	0.99	83	
22	Average	0.31	19	0.31	19	0.46	27	0.65	34	0.76	42	0.85	46	0.90	50	



Fig. 3. Comparison of visual results ($QP=37$). The 1st row : The 193th frame of *BQMall* video. The 2nd row: The 19th frame of *RaceHorses* video. The 3rd row: The 168th frame of real-world compressed video-1. The 4th rows: The 1,082th frame of real-world compressed video-2.

TABLE II
ABLATION STUDY AT $QP=37$ WITH STDF AS BASELINE

IntraGFA+InterGFF	FE	Δ PSNR (dB)	Δ SSIM ($\times 10^{-4}$)
-	-	0.77	139
✓	-	0.88	160
✓	✓	0.96	177

II that IntraGFA and InterGFF modules obtain 0.11dB Δ PSNR gain (on average) over the baseline, which demonstrates their effectiveness. Besides, we introduce our FE module with three SDCBs to the combined IntraGFA and InterGFF modules to construct our proposed model. It is found from Table II that introducing the FE module obtains further improves the performance, demonstrating its effectiveness.

In addition, we verify the effectiveness of the number of designed SDCB. Specifically, we use one SDCB and two SDCBs to construct two corresponding models, denoted as *Ours-1* and *Ours-2*, respectively. The corresponding results are given in Table III. It is found from Table III that the method *Ours-1* i.e., using one SDCB, performs better than RFDA and CF-STIF, as proved by the achieved higher performance gain. In addition, the method *Ours-2*, i.e., using two SDCBs,

TABLE III

VERIFICATION OF USING DIFFERENT NUMBERS OF SDCB AT $QP=37$

	Δ PSNR (dB)	Δ SSIM ($\times 10^{-4}$)	Param. (K)
Ours-1	0.92	169	1251
Ours-2	0.94	173	1327
Ours	0.96	177	1403

TABLE IV

COMPARISON OF PARAMETERS, FLOPS AND INFERENCE SPEED (FPS)

	Param.(K)	FLOPs(G)	FPS @Different Resolution		
			Class C	Class D	Class E
STDF-R3L	1275	83.5	17.37	37.03	4.24
RFDA	1270	56.8	15.41	32.14	3.74
CF-STIF	2200	194.6	9.16	26.32	2.05
Ours	1403	143.2	11.00	28.54	2.43

performs better than *Ours-1*, which indicates that using more SDCBs can effectively improve the enhancement performance.

5) *Complexity Comparison*: We provide model parameters, FLOPs, and inference speed of our method and three comparable methods, i.e., STDF-R3L, RFDA and CF-STIF, in Table IV, where all the compared methods adopt 7 successive frames to generate enhanced video. The FLOPs are calculated on the Class-D video and the inference speed is evaluated in terms of the frame per second (FPS). It is found from Table IV that our method achieves fewer parameters and FLOPs, but higher inference speed than CF-STIF. Although our method is more complicated than STDF-R3L and RFDA, it is still competitive for practical applications due to the higher enhancement performance.

IV. CONCLUSION

In this paper, we proposed temporal group alignment and fusion network to enhance the quality of compressed video. With our proposed model, the long-short term correlations between frames are explored to generate effective features to compose high-quality videos. The complexity of our method accordingly increases due to extracting these features, which will limit the application efficiency of our method. We will focus on the design of low-complexity modules for our enhancement model in the future work.

REFERENCES

- [1] K. Seshadrinathan, R. Soundararajan, A. C. Bovik, and L. K. Cormack, "Study of subjective and objective quality assessment of video," *IEEE Trans. Image Process.*, vol. 19, no. 6, pp. 1427–1441, Jun. 2010.
- [2] T. Keng Tan, R. Weerakkody, M. Mrak, N. Ramzan, V. Baroncini, J. Ohm, and Gary J. Sullivan, "Video quality evaluation methodology and verification testing of HEVC compression performance," *IEEE Trans. Circuits Syst. Video Technol.*, vol. 26, no. 1, pp. 76–90, Jan. 2016.
- [3] C. G. Bampis, Z. Li, A. K. Moorthy, I. Katsavounidis, A. Aaron, and A. C. Bovik, "Study of temporal effects on subjective video quality of experience," *IEEE Trans. Image Process.*, vol. 26, no. 11, pp. 5217–5231, Nov. 2017.
- [4] R. Yang, H. Liu, S. Zhu, X. Zheng, and B. Zeng, "DFCE: Decoder-friendly chrominance enhancement for HEVC intra coding," *IEEE Trans. Circuits Syst. Video Technol.* vol. 33, no. 3, pp. 1481–1486, Mar. 2023.
- [5] T. Wang, M. Chen, and H. Chao, "A novel deep learning-based method of improving coding efficiency from the decoder-end for HEVC," in *Proc. Data Compression Conf.*, 2017, pp. 410–419.
- [6] R. Yang, M. Xu, T. Liu, Z. Wang, and Z. Guan, "Enhancing quality for HEVC compressed videos," *IEEE Trans. Circuits Syst. Video Technol.*, vol. 29, no. 7, pp. 2039–2054, Jul. 2019.
- [7] Z. Pan, W. Yu, J. Lei, N. Ling, and S. Kwong, "TSAN: Synthesized view quality enhancement via two-stream attention network for 3D-HEVC," *IEEE Trans. Circuits Syst. Video Technol.*, vol. 32, no. 1, pp. 345–358, Jan. 2022.
- [8] Z. Pan, F. Yuan, W. Yu, J. Lei, N. Ling, and S. Kwong, "RDEN: Residual distillation enhanced network-guided lightweight synthesized view quality enhancement for 3D-HEVC," *IEEE Trans. Circuits Syst. Video Technol.*, vol. 32, no. 9, pp. 6347–6359, Sept. 2022.
- [9] R. Yang, M. Xu, Z. Wang, and T. Li, "Multi-frame quality enhancement for compressed video," in *Proc. IEEE Conf. Comput. Vision Pattern Recognit.*, 2018, pp. 6664–6673.
- [10] Z. Guan, Q. Xing, M. Xu, R. Yang, T. Liu, and Z. Wang, "MFQE 2.0: A new approach for multi-frame quality enhancement on compressed video," *IEEE Trans. Pattern Anal. Mach. Intell.*, vol. 43, no. 3, pp. 949–963, Mar. 2021.
- [11] J. Deng, L. Wang, S. Pu, and C. Zhuo, "Spatio-temporal deformable convolution for compressed video quality enhancement," in *Proc. AAAI Conf. Artif. Intell.*, vol. 34, no. 7, 2020, pp. 10696–10703.
- [12] M. Zhao, Y. Xu, and S. Zhou, "Recursive fusion and deformable spatiotemporal attention for video compression artifact reduction," in *Proc. ACM Int. Conf. Multi.*, 2021, pp. 5646–5654.
- [13] D. Luo, M. Ye, S. Li, C. Zhu, and X. Li, "Spatio-temporal detail information retrieval for compressed video quality enhancement," *IEEE Trans. Multi.* pp. 1-14, Oct. 2022.
- [14] L. Yu, W. Chang, S. Wu and M. Gabbouj, "End-to-end transformer for compressed video quality enhancement," *IEEE Trans. Broadcast.*, vol. 70, no. 1, pp. 197-207, Mar. 2024.
- [15] M. Yang, X. Zhou, F. Yang, M. Zhou, and H. Wang, "PIMnet: A quality enhancement network for compressed videos with prior information modulation," *Signal Process: Image Communication*, pp. 117005, Sep. 2023.
- [16] Y. Xiao, Q. Yuan, Q. Zhang, and L. Zhang, "Deep blind super-resolution for satellite video," *IEEE Trans. Geosci. Remote Sens.*, vol. 61, pp. 1-16, 2023.
- [17] Y. Xiao, Q. Yuan, K. Jiang, X. Jin, J. He, L. Zhang, and C. -W. Lin, "Local-global temporal difference learning for satellite video super-resolution," *IEEE Trans. Circuits Syst. Video Technol.* vol. 34, no. 4, pp. 2789-2802, Apr. 2024.
- [18] Y. Xiao, X. Su, Q. Yuan, D. Liu, H. Shen and L. Zhang, "Satellite video super-resolution via multiscale deformable convolution alignment and temporal grouping projection," *IEEE Trans. Geosci. Remote Sens.*, vol. 60, pp. 1-19, 2022.
- [19] K. Jiang, Z. Wang, P. Yi, T. Lu, J. Jiang, and Z. Xiong, "Dual-path deep fusion network for face image hallucination," *IEEE Trans. Neural Netw. Learn. Syst.*, vol. 33, no. 1, pp. 378-391, Jan. 2022.
- [20] K. Jiang, Z. Wang, P. Yi, C. Chen, Z. Wang, X. Wang, J. Jiang, and C. -W. Lin, "Rain-free and residue hand-in-hand: A progressive coupled network for real-time image deraining," *IEEE Trans. Image Process.*, vol. 30, pp. 7404-7418, 2021.
- [21] O. Ronneberger, P. Fischer, and T. Brox, "U-Net: convolutional networks for biomedical image segmentation," in *Proc. Int. Conf. Medical Image Comput. and Computer-Assisted Interv.* Springer, 2015, pp. 234–241.
- [22] J. Dai, H. Qi, Y. Xiong, Y. Li, G. Zhang, H. Hu, and Y. Wei, "Deformable convolutional networks," in *Proc. IEEE Int. Conf. Comput. Vision*, 2017, pp. 764–773.
- [23] J.-R. Ohm, G. J. Sullivan, H. Schwarz, T. K. Tan, and T. Wiegand, "Comparison of the coding efficiency of video coding standards-including high efficiency video coding (HEVC)," *IEEE Trans. Circuits Syst. Video Technol.*, vol. 22, no. 12, pp. 1669–1684, 2012.
- [24] G. J. Sullivan, J.-R. Ohm, W.-J. Han, and T. Wiegand, "Overview of the high efficiency video coding (HEVC) standard," *IEEE Trans. Circuits Syst. Video Technol.*, vol. 22, no. 12, pp. 1649–1668, Dec. 2012.
- [25] D. Kingma and J. Ba, "Adam: A method for stochastic optimization," in *Proc. Int. Conf. Learn. Representations*, 2015. [Online]. Available: <https://arxiv.org/abs/1412.6980v9>
- [26] D. Luo, M. Ye, S. Li, and X. Li, "Coarse-to-fine spatio-temporal information fusion for compressed video quality enhancement," *IEEE Signal Process. Lett.*, vol. 29, pp. 543–547, 2022.
- [27] Y. Zhang, K. Li, K. Li, L. Wang, B. Zhong, and Y. Fu. "Image super-resolution using very deep residual channel attention networks," in *Proc. of the Eur. Conf. on Computer Vision*. pp. 286–301, Sep. 2018.
- [28] S. Zamir, A. Arora, S. Khan, M. Hayat, F. Khan, M. Yang, and L. Shao, "Learning enriched features for fast image restoration and enhancement," *IEEE Trans. Pattern Anal. Mach. Intell.* vol. 45, no. 2, pp. 1934–1948, Feb. 2023.
- [29] W. -S. Lai, J. -B. Huang, N. Ahuja, and M. -H. Yang, "Fast and accurate image super-resolution with deep laplacian pyramid networks," *IEEE Trans. Pattern Anal. Mach. Intell.*, vol. 41, no. 11, pp. 2599-2613, Nov. 2019.